Simple characterization of electronic processes in perovskite photovoltaic cells

Kenjiro Miyano,[a] Masatoshi Yanagida, Neeti Tripathi, and Yasuhiro Shirai
Global Research Center for Environment and Energy Based on Nanomaterials Science (GREEN), National Institute for Materials Science (NIMS), 1-1 Namiki, Tsukuba, Ibaraki 305-0044, Japan

(Received 14 December 2014; accepted 23 February 2015; published online 4 March 2015)

Electronic properties of perovskite lead-halide photovoltaic cells have been studied. The *dc* current/voltage characteristics were found to be well fitted by a standard diode equation under optical excitation and in the dark, while the impedance spectroscopy revealed a pronounced slow process under light illumination, which is absent in the dark. A simple model is proposed, which can explain all aspects of the observed behavior quantitatively and consistently. © *2015 AIP Publishing LLC*. [http://dx.doi.org/10.1063/1.4914086]

The last few years have witnessed numerous studies on photovoltaic (PV) cells based on lead-iodide perovskite ($MAPbI_3$, MA = methyl ammonium) or related compounds.[1–3] Although the current surge of research has begun with the proposal of using perovskite as a sensitizer in a dye-sensitized solar cell,[4] the prevailing viewpoint is that the material behaves as a photocurrent generator and a carrier conductor at the same time, just like an active region in a conventional inorganic semiconductor PV cell. In this case, the simplest model of a perovskite PV cell is a *pin* diode with *i* being the perovskite layer and *p* and *n* carrier selecting contacts. Because of the band structure, $MAPbI_3$ can be an ideal ambipolar intrinsic semiconductor.[5] In this letter, we present results on current/voltage (*J*/*V*) measurements and impedance spectroscopy (IS) of perovskite PV cells in the dark and under illumination. By employing good quality samples, very simple and quantitatively analyzable picture emerges; the *J*/*V* measurements are perfectly consistent with a simple diode model and the IS under light illumination showed a very slow process reminiscent of hopping conduction.

Samples were fabricated using a two-step inter-diffusion method with the second step administered by dynamic dispensing.[6] The cell structure is ITO/PEDOT:PSS/$MAPbI_3$/$PC_{61}BM$/Ca/Ag (ITO = tin-doped indium oxide, PEDOT:PSS = Poly(3,4-ethylenedioxythiophene):Poly(styrenesulfonate), $PC_{61}BM$ = Phenyl-C_{61}-Butyric-Acid-Methyl Ester). We should point out two essential factors of our samples[7,8] that enabled us to extract the simple picture stated above. (1) The cell structure is planar. Higher efficiency has generally been reported with cells with mesoporous oxide layers. However, our priority was to avoid the potential difficulties in defining equipotential plane in the mesoporous structure in interpreting the *J*/*V* data and in assuming the effective dielectric constant of the oxide/perovskite complex in analyzing the IS data. (2) Care was taken to prepare samples without hysteresis. Otherwise, the *J*/*V* measurements are clearly meaningless and low frequency IS has complication due to the slow process. This will be further discussed later.

Our proposition was first tested by comparing the *J*/*V* behavior against the standard diode model depicted in Fig. 1(a). In this model, the current (*J*)-voltage (*V*) relationship at the device terminals is expressed by the following equation:

$$J(V) = J_{ph} - J_0\left[\exp\left(\frac{eV + JR_s}{nk_BT}\right) - 1\right] - \frac{V + JR_s}{R_{sh}}, \quad (1)$$

where J_{ph} is the photogenerated current density, J_0 the reverse saturation current density, e the elementary charge, R_{sh} the shunt resistance, R_s the series resistance, k_B the Boltzmann constant, T the absolute temperature, and n the ideality factor.

In Fig. 2, we show typical data with fitting results for a device that shows 11.5% conversion efficiency. The fitting has been done by minimizing the sum of the relative error, $\sum(|J_{calculated} - J_{data}|/|J_{data}|)$ through an iterative procedure. Only four representative curves are shown for clarity. Over the wide range of illumination intensity of 0% sun to 100% sun (=100 mW/cm^2) and over the entire voltage range, the average relative error is about 1%. The fitted ideality factor is $n = 1.29$. We did not use the standard least-squares method here because of the error in fitting the low illumination data. Details are given in the supplementary material.[8]

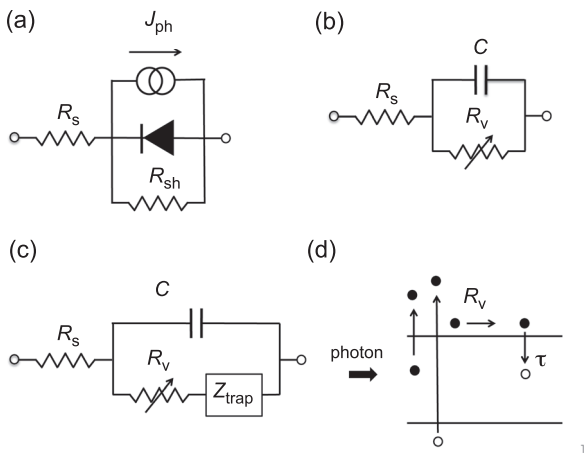

FIG. 1. (a) A standard diode model. J_{ph}: photogenerated current density, R_{sh}: shunt resistance, R_s: series resistance. (b) Equivalent circuit of the cell in the dark for the IS analysis. C: Capacitance, R_v: variable resistance. (c) Equivalent circuit of the cell under illumination for the IS analysis. Z_{trap} depicts dispersive resistance element. (d) Schematic presentation of the proposed electronic processes involving the trapping and photoinduced detrapping of the carriers.

[a]MIYANO.Kenjiro@nims.go.jp

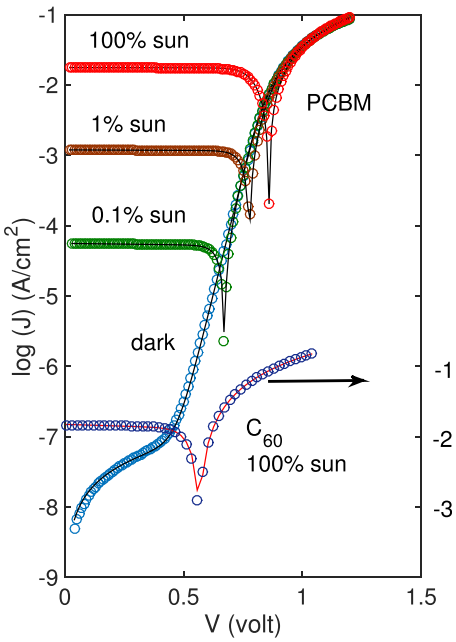

FIG. 2. *J*/*V* plot and fit to the data using Eq. (1). For the cell with a PCBM electron transport layer, representative curves at four different illumination intensities are shown. For the data of C_{60} electrode cell, only one curve at 100% sun is shown. The baseline is shifted for clarity.

The ideality factor is usually associated with the carrier recombination process, understanding of which is imperative to reduce the efficiency loss. One scenario extensively studied is the recombination centers in the space charge region of a *pn* junction.[9] The deep trap states lying near the quasi-Fermi energy are efficient recombination centers resulting in complex recombination behavior depending on the operation point of the diode. In a *pin* diode, a similar consideration is appropriate to the *i* layer, i.e., the perovskite bulk in our case. Another concern is the surface recombination through the surface states.

In order to gain insight into the surface effect, we studied *J*/*V* relationship with a different contact material. We replaced the $PC_{61}BM$ layer of the initial design by C_{60} layer resulting in two physical modifications; the mobility increases and LUMO deepens.[10,11] In accordance with these changes, V_{oc} decreased by about 0.3 V due to the LUMO shift while R_s improved from 3.0 $\Omega\cdot cm^2$ to 2.6 $\Omega\cdot cm^2$ (Fig. 2). Although the efficiency is much lower due to the low V_{oc}, the ideality factor is not much different, $n = 1.28$.

The absence of a noticeable change in n by replacing the contact material may imply that the surface (interface) traps do not contribute much to the recombination. However, we found that n is not a sensitive indicator of the device quality in perovskite PVs. As an example, we show in Fig. 3 the fitting results of two devices with different fill-factors (FFs). The FF and the efficiency (η) are shown in the legend. The fitting was done here by the usual least-squares method so that the standard deviation (σ in the figure) can be discussed. (Please refer to the supplementary materials for detailed discussion.[8]) The fitted n are the same in both samples and, at

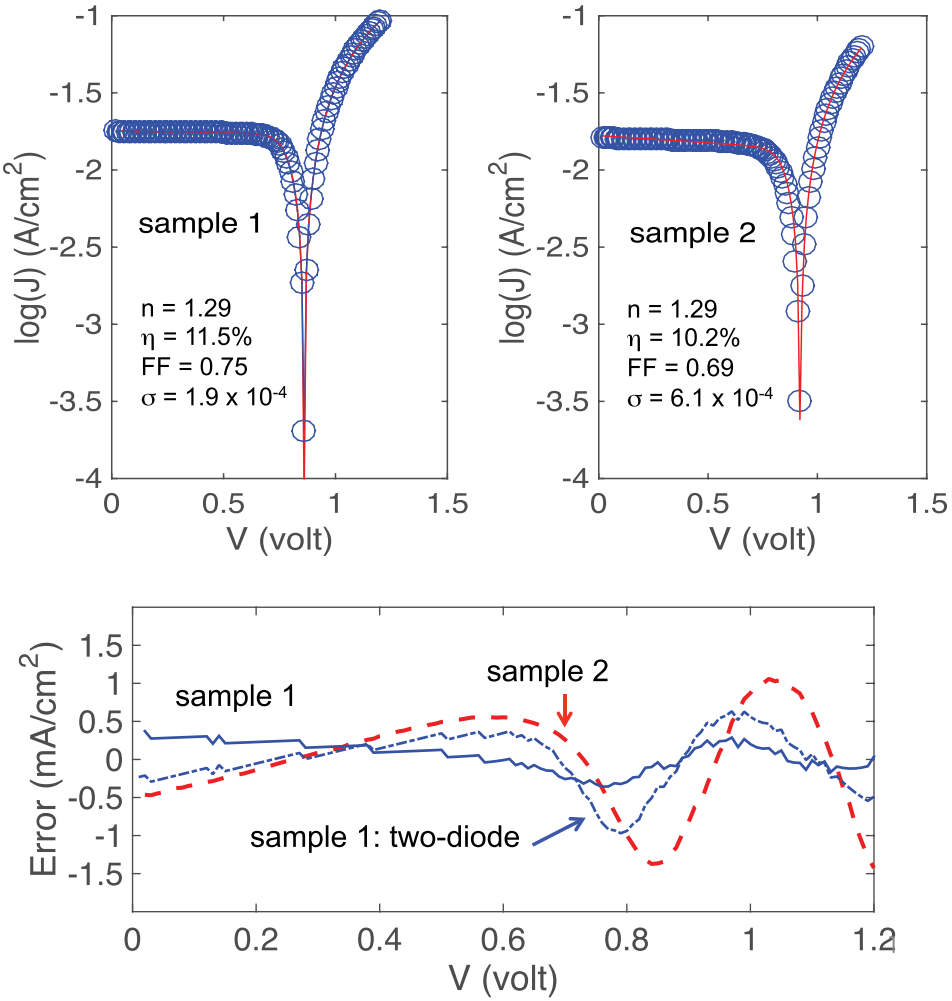

FIG. 3. (Top two panels) Fit to the *J*/*V* curves of two devices (samples 1 and 2). (Bottom panel) The error of the fit for sample 1 (solid line) and sample 2 (dashed line). The error of the fit of sample 1 using the two-diode model is also shown (dotted-dashed line).

first glance, the fitting is equally good. However, the standard deviation of the fit for sample 2 ($\sigma = 6.1 \times 10^{-4}$ A/cm^2) is considerably worse than that of sample 1 ($\sigma = 1.9 \times 10^{-4}$ A/cm^2). The difference becomes obvious when we plot the error (J_{data}–$J_{calculated}$) (bottom panel of Fig. 3). Let us note that the error is systematic rather than random, i.e., some physical processes escaped our analysis.

We found that our samples with reasonable quality (typically FF better than 0.7 and hysteresis-free (quantified later)) show invariably $n \sim 1.3$. Furthermore, as the error (Fig. 3, bottom panel) indicates, the better the samples are, the better they are represented by the standard diode equation. The real cause of the efficiency loss is from different kind of sources not represented by the diode equation. Incidentally, another widely used model, the two-diode model with a combination of $n = 1$ and $n = 2$,[12] does not produce better fit ($\sigma = 3.5 \times 10^{-4}$ in sample 1) as shown in Fig. 3, bottom panel. Interestingly, the error for one-diode model and that for two-diode model are qualitatively similar except for the goodness of the fit. From this observation, we tentatively conclude that the one-diode model is more appropriate, although more exhaustive study is clearly desired.

In order to look into the transport processes not considered in Eq. (1), we performed IS measurements. The impedance was measured from 0.1 Hz to 1 MHz with an *ac* modulation of 10 mV amplitude. The measurement setup has a 10 Ω input impedance in the current-to-voltage conversion process. In the following, the raw data including this input impedance are presented rather than the background-subtracted and area-normalized values as done in Figs. 2 and 3. In the J/V measurements, the active irradiated area is defined by placing a mask above the cell surface. However, in the impedance measurement, the entire junction area is inevitably involved, which is less accurately measured. The uncertainty is estimated to be about 10%.

Typical Nyquist plots in the dark are shown in Figs. 4(a) and 4(b), whose equivalent circuit is shown in Fig. 1(b). At 0 V bias, the resistance R_v is very large ($R_{sh} \sim$ a few hundred

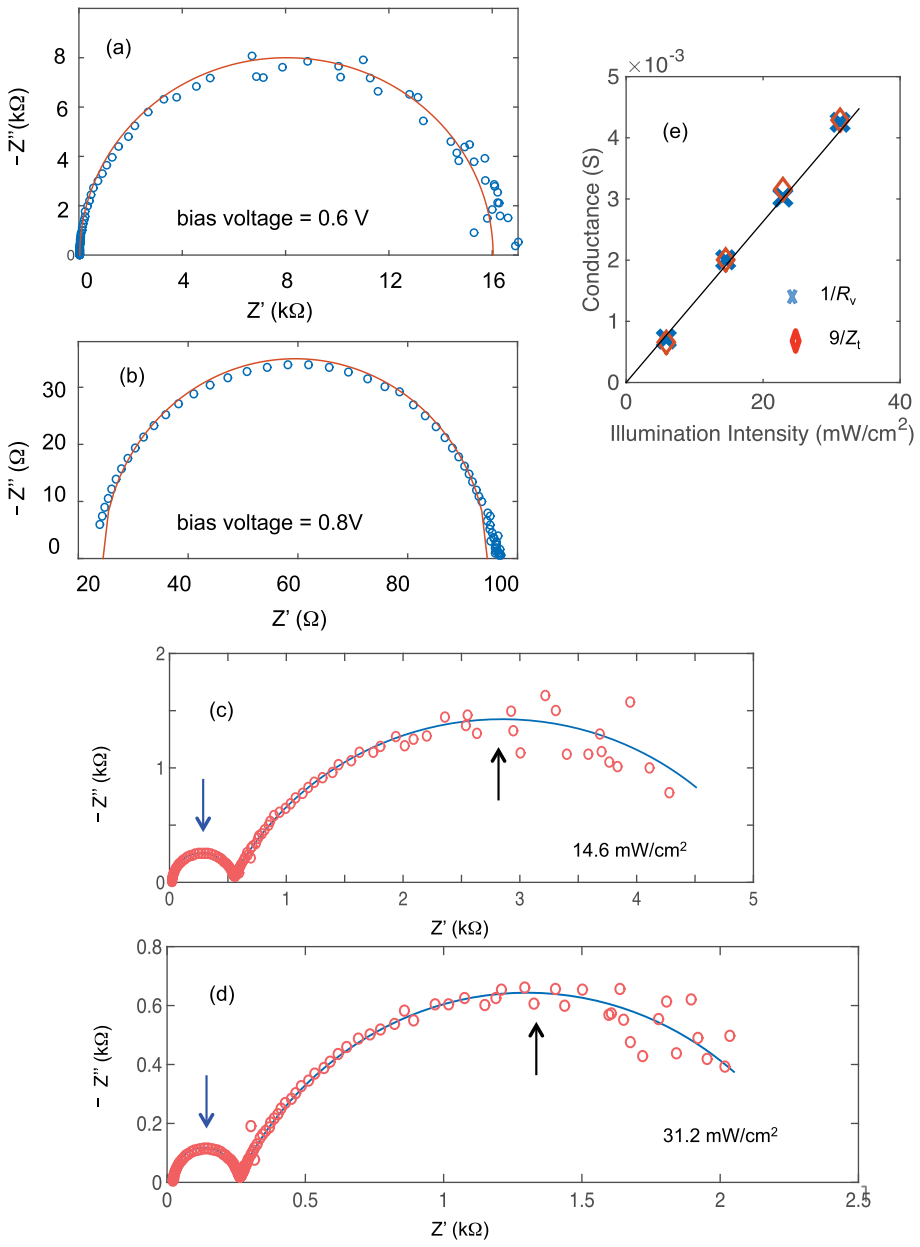

FIG. 4. Nyquist plots of the cell in the dark at bias voltage of (a) 0.6 V and at (b) 0.8 V. Nyquist plots of the cell at zero bias voltage with light illumination of (c) 14.6 mW/cm^2 and (d) 31.2 mW/cm^2. (e) $1/R_v$ (crosses) and $9/Zt$ (diamonds) vs. light illumination intensity (Eq. (3)). The line is a guide to the eye.

kΩ) and the circuit behaves as if a pure capacitor with a series resistor R_s. From the measured capacitance ($C = 15$ nF), we arrive at the relative permittivity ε_r of about 22. The value is in reasonable agreement with a recent publication.[13]

As the forward bias voltage is increased, the semicircle gets smaller. The shape is defined by the high-frequency resistance of R_s and low-frequency resistance (R_v in Fig. 1(b)). The R_s measured here with the input impedance and the junction surface area corrections agrees well with the one obtained by the J/V curve fitting. R_v agrees with the differential resistance $(dJ/dV)^{-1}$ of the J/V curve. The equivalent circuit at finite bias voltage thus behaves as is expected from the *dc* J/V curve. From the frequency at the top of the semicircle, capacitance is calculated at each bias voltage, which shows some forward bias dependence. The Mott-Schottky (MS) plot $(1/C^2\, vs\, V)$ indicates that the so-called chemical capacitance (the density of states contribution[14]) is small; reasonable because the relevant gap here is between the bulk band states. The MS plot, however, shows a small change in the slope around $V \sim 0.4$ V. This implies that the space charge effect is masked by the large dielectric constant of $MAPbI_3$ at zero bias and the measured capacitance is mostly due to the intrinsic dielectric constant of the material, as was noted above.

The Nyquist plot under light illumination is completely different, as shown in Figs. 4(c) and 4(d). It now consists of two semicircles, whose sizes systematically shift to lower values as the light intensity increases. The two well separated semicircles imply that there are two resistive elements connected in series, i.e., the two impedance elements are additive. From the observation that the higher frequency circle is semicircular but the lower frequency circle is substantially flattened, we must ascribe the former to a simple parallel resistance-capacitance (*RC*) element and the latter to a dispersive process; most likely hopping conduction assisted by photoexcitation. This is illustrated in Fig. 1(c), in which the hopping impedance is depicted as Z_{trap}.

The two resistive elements must not be physically separated in the $MAPbI_3$ layer, since there is no obvious way to cut the cell into two physically distinct regions along the cell normal. Therefore, we reason as follows. At zero bias voltage, the *dc* differential impedance $(dJ/dV)^{-1}$ is still very large even under illumination. However, Figs. 4(c) and 4(d) indicate that there is a current component that cannot immediately adjust the *ac* voltage modulation aside from the capacitance charge-discharge current due to the large material permittivity. Because the cell behaves as an ordinary *RC* circuit (Fig. 1(b)) under external carrier injection from the electrodes in the dark (Figs. 4(a) and 4(b)), the behavior under light illumination should be associated with the nature of the carriers present in the perovskite under illumination. Carriers are continuously generated and extracted from the electrodes at 0 V bias. The photoexcitation not only creates electrons and holes in the conduction and valence bands but also activates deep traps, which is an additional process absent in the conduction in the dark. The photoassisted trapping-detrapping process is slow so that it cannot respond to the *ac* voltage modulation. The time constant associated with this process depends on parameters such as the energy level and trapping cross-section. Because many types of traps are likely to coexist, a distribution function of the trap time is required, which is difficult to determine. A customary procedure to describe the trapping-detrapping conduction is to assume a Gaussian distribution of trap levels,[15] which results in an impedance response in the form of stretched exponential

$$Z_{\text{trap}} = Z_t/(1 + (i\omega\tau)^{\alpha}), \tag{2}$$

where τ is the characteristic time constant and α the exponent.

In Figs. 4(c) and 4(d), the fitted results using Eq. (2) are also shown. Note here that we used the same C and R_s values of the device in the dark at zero bias. The top of the semicircles indicated by the downward arrows corresponds to $C = 1/\omega \cdot R_v$, from which R_v is calculated. The exponent $\alpha = 0.7$ and the characteristic time constant that corresponds to the top of the arc (upward arrows in Figs. 4(c) and 4(d)) is $\tau \sim 0.1$ s independent of the light intensity. Of course, the pure resistive and hopping processes are not physically separated as the equivalent circuit (Fig. 1(c)) might imply. Carrier trapping-detrapping and drift occur everywhere in the sample but they are sequential (Fig. 1(d)). The basic process that occurs between hopping events is carrier drift, whose conductance is given by

$$\sigma \sim \mu n_c \sim 1/R_v \sim 1/Z_t, \tag{3}$$

where μ is the mobility and n_c the carrier density. Because the carrier density is proportional to the illumination intensity, the resistive parameters in Fig. 1(c), R_v and Z_t (Eq. (2)) should be inversely proportional to the light intensity. In Fig. 4(e), we show $1/R_v$ and $9/Z_t$ as functions of light illumination intensity. The factor 9 in the latter is simply to bring the two values in the same range for clarity although it is not known if there is any physical significance in the value or not.

Before closing, some comments on our results with respect to the published data are in order. Earlier works on the J/V curve fitting and extraction of the ideality factor have been done by reading the slope from a part of $\log(J)/V$ plot,[16,17] which is not totally free from arbitrariness in the choice of the voltage range. The recent analysis is more complete,[18] although the quality of the fit is not described and the superposition principle appears to be not applicable because the J/V curve in the dark crosses that under illumination. In contrast, we have shown that a complete fit to an analytical expression is possible, through which we found, for example, the bending at higher current in our case is due to the R_s rather than the space charge limited transport in the HTL (hole transport layer).[16] Finding an analytical expression is not academic curiosity; without it, the analysis of a tandem device (perovskite has been considered as a top cell in a tandem device), is not possible.[12]

Our Nyquist plots (Fig. 4) differ considerably from those published previously. Particularly, we do not observe the behavior that hints the presence of the Warburg-type element.[19] We suspect that the hysteretic behavior of the J/V curve affects the IS measurement at low frequencies because it has typical diffusive behavior; the slower the scan is the larger the hysteresis becomes.[20] In this respect, the Nyquist

plot of a sample, in which the hysteresis is simultaneously measured is particularly interesting and needs further analysis, because the *J*/*V* scan rate of 1 V/s is comparable to the 10 mV modulation at 0.01 Hz in the IS measurement.[21] The contribution of the HTL is also discussed forming series circuit to the perovskite layer.[22] In our cell, the resistance of HTL is very low: from the bulk conductivity of the PEDOT:PSS used, its contribution to R_s is 5 mΩ cm^2. In any case, R_s as a whole is too small ($1/R_sC \sim \omega$ too high frequency) to affect the Nyquist plot in the frequency range of our measurement.

Finally, we emphasize that our samples do not show hysteresis. More quantitatively, in terms of a parameter, the hysteresis index ($HI = (J_{RS}(0.8V_{oc}) - J_{FS}(0.8V_{oc})/J_{RS}(0.8V_{oc})$) proposed in Ref. 23, measurements reported here are done using samples with IH better than 5%.[7] In the *J*/*V* curve fitting, described above, we showed that the error of the fit is about 1%. It is obviously meaningless to try to seek a better fit in the presence of the hysteresis worse than twice the fitting error. As for the Nyquist plot, the salient feature of Fig. 4 is the simplicity and quantitative fit. The equivalent circuits, Figs. 1(b) and 1(c), can explain the Nyquist plots shown in Figs. 4(a)–4(d), respectively, using only tow parameters $C = 15$ nF and $\alpha = 0.7$, together with the numbers read from the *J*/*V* curves.

In conclusion, we have shown that *J*/*V* relationship and IS in the dark and under illumination are described very well by a simple model depicted in Fig. 1 together with the diode equation (Eq. (1)) and the hopping conduction (Eq. (2)) augmented by the drift conductance (Eq. (3)). All of our data can be well fitted quantitatively using the same set of parameters without any additional assumptions. Although the physical meanings of n, α, and τ are yet to be explained, we believe that we have a solid ground to do systematic quantitative study of perovskite PVs, which will lead to better understanding of the electronic processes and useful device development. A more exhaustive study is underway.

This research has been supported, in part, by MEXT Program for Development of Environmental Technology using Nanotechnology (GREEN). We are grateful to Dr. L. Han for his generous support in providing us with the experimental facilities.

[1]P. P. Boix, K. Nonomura, N. Mathews, and S. G. Mhaisalkar, Mater. Today **17**, 16 (2014).
[2]T. C. Sum and N. Mathews, Energy Environ. Sci. **7**, 2518 (2014).
[3]B. Wang, X. Xiao, and T. Chen, Nanoscale **6**, 12287 (2014).
[4]A. Kojima, K. Teshima, Y. Shirai, and T. Miyaska, J. Am. Chem. Soc. **131**, 6050–6051 (2009).
[5]J. Even, L. Pedesseau, M.-A. Dupertuis, J.-M. Jancu, and C. Katan, Phys. Rev. B **86**, 205301 (2012).
[6]Z. Xiao, C. Bi, Y. Shao, Q. Dong, Q. Wang, Y. Yuan, C. Wang, Y. Gao, and J. Huang, Energy Environ. Sci. **7**, 2619 (2014).
[7]N. Tripathi, M. Yanagidaa, Y. Shirai, T. Masuda, L. Han, and K. Miyano, "Stable and reproducible planar perovskite/$PC_{61}BM$ solar devices with improved performance via chlorine mediated two step diffusion method," ACS Appl. Mater. Interfaces (submitted).
[8]See supplementary material at http://dx.doi.org/10.1063/1.4914086 for a complete derivation.
[9]C.-T. Sah, R. N. Noyce, and W. Schockley, Proc. IRE **45**, 1228 (1957).
[10]C.-Z. Li, H.-L. Yip, and A. K.-Y. Jen, J. Mater. Chem. **22**, 4161 (2012).
[11]K. Akaike, K. Kanai, H. Yoshida, J. Tsutsumi, T. Nishi, N. Sato, Y. Ouchi, and K. Seki, J. Appl. Phys. **104**, 023710 (2008).
[12]T. Sogabe, A. Ogura, C.-Y. Hung, V. Evstropov, M. Mintairov, M. Shavarts, and Y. Okada, Appl. Phys. Lett. **103**, 263907 (2013).
[13]M. Samiee, S. Konduri, B. Ganapathy, R. Kottokkaran, H. A. Abbas, A. Kitahara, P. Joshi, L. Zhang, M. Noack, and V. Dalal, Appl. Phys. Lett. **105**, 153502 (2014).
[14]J. Bisquert, Phys. Chem. Chem. Phys. **5**, 5360 (2003).
[15]S. Havriliak and S. Negami, Polymer **8**, 161 (1967).
[16]S. Agarwal, M. Seetharaman, N. K. Kumawat, A. S. Subbiah, S. K. Sarkar, D. Kabra, M. A. G. Namboothiry, and P. R. Nair, J. Phys. Chem. Lett. **5**, 4115 (2014).
[17]J. Shi, J. Dong, S. Lv, Y. Xu, L. Zhu, J. Xiao, X. Xu, H. Wu, D. Li, Y. Luo, and Q. Meng, Appl. Phys. Lett. **104**, 063901 (2014).
[18]H. Wei, J. Shi, X. Xu, J. Xiao, J. Luo, J. Dong, S. Lv, L. Zhu, H. Wu, D. Li, Y. Luo, Q. Meng, and Q. Chen, Phys. Chem. Chem. Phys. **17**, 4937–4944 (2015).
[19]H. S. Kim, I. Mora-Sero, V. Gonzalez-Pedro, F. Fabregat-Santiago, E. J. Juarez-Perez, N. G. Park, and J. Bisquert, Nat. Commun. **4**, 2242 (2013).
[20]H. J. Snaith, A. Abate, J. M. Ball, G. E. Eperon, T. Leijtens, N. K. Noel, S. D. Stranks, J. T.-W. Wang, K. Wojciechowski, and W. Zhang, J. Phys. Chem. Lett. **5**, 1511 (2014).
[21]R. S. Sanchez, V. Gonzalez-Pedro, J.-W. Lee, N.-G. Park, Y. S. Kang, I. Mora-Sero, and J. Bisquert, J. Phys. Chem. Lett. **5**, 2357 (2014).
[22]J. A. Christians, R. C. M. Fung, and P. V. Kamat, J. Am. Chem. Soc. **136**, 758 (2014).
[23]H.-S. Kim and N.-G. Park, J. Phys. Chem. Lett. **5**, 2927 (2014).